

Influence of Defect Identification Method on the Statistics of Primary Irradiation Damage in α -Zirconium

K. P. Boyle and T. J. Robotham

CanmetMATERIALS, Natural Resources Canada, Hamilton, ON, Canada
(kboyle@nrcan.gc.ca)

Abstract

Molecular dynamics simulations are used to study primary irradiation damage in α -Zr as a function of incident recoil energy and temperature. Previous studies have concluded that the number of stable defects generated from displacement cascades in α -Zr is temperature independent. A new approach for identifying defects, based on temperature-dependent search radius, is developed. Our results contrast with previous studies, as defect production in α -Zr is revealed to be strongly temperature dependent. The number of defects generated was found to decrease with increasing temperature, although this decrease appears to saturate at 600 K. Based on the findings, an equation for defect generation which accounts for the influence of temperature and recoil energy is proposed.

1. Introduction

Zirconium alloys are important for the Canadian nuclear industry as they are used for various structural components in current nuclear reactor systems. Although zirconium alloys offer exceptional neutron transparency and adequate mechanical strength at the operating temperatures of interest, they are susceptible to degradation phenomena associated with irradiation damage, including irradiation creep [1-4] and irradiation growth [5-7]. Understanding these irradiation driven degradation phenomena is critical for assessment and life-time predictions of in-core reactor components.

The underlying mechanism of irradiation damage lies in the evolution of defects induced by the neutron-incited displacement cascade, which produces excess vacancies and self-interstitial atoms (SIAs). Due to the time and length scales involved in the primary irradiation damage process, molecular dynamics simulations are often used to study various aspects of irradiation-induced damage. Molecular dynamics studies of primary irradiation damage in α -Zr have primarily focused on the influence of incident neutron energy and base lattice temperature on defect production [8-11]. Defect generation data, as measured by the final number of Frenkel pairs N_F , is compiled from various sources [9-11] and shown in Fig. 1 as a function of primary knock-on atom (PKA) energy E_p . The majority of α -Zr displacement cascade studies, including those cited above, have used the AWB95 interatomic potential [12].

The data presented in Fig. 1 can be fit to a linear relation. This is consistent with the often used NRT model [13], for which N_F is taken to be proportional to the damage energy. In molecular

dynamics simulations, all of the PKA energy is available to generate atomic displacement by elastic collisions and therefore the damage energy can be replaced by E_p , which suggests the simulation results can be described by,

$$N_F = A E_p + N_o \quad (1)$$

where slope A and intercept N_o have the usual meaning and E_p must be greater than about twice the threshold displacement energy E_d . Although Gao and co-workers [10] observed temperature-dependent defect generation, i.e. a difference in the number of defects generated at 100 versus 600 K as reproduced in Fig. 1 below, the temperature dependence is small and is usually ignored. A linear regression of the data, assuming temperature independence, leads to parameter values $A = 2.2$ and $N_o = 1.8$.

The objective of the current work is to determine how the method used for identifying irradiation defects influences the statistics and the temperature dependence of primary irradiation generation for displacement cascades in α -Zr.

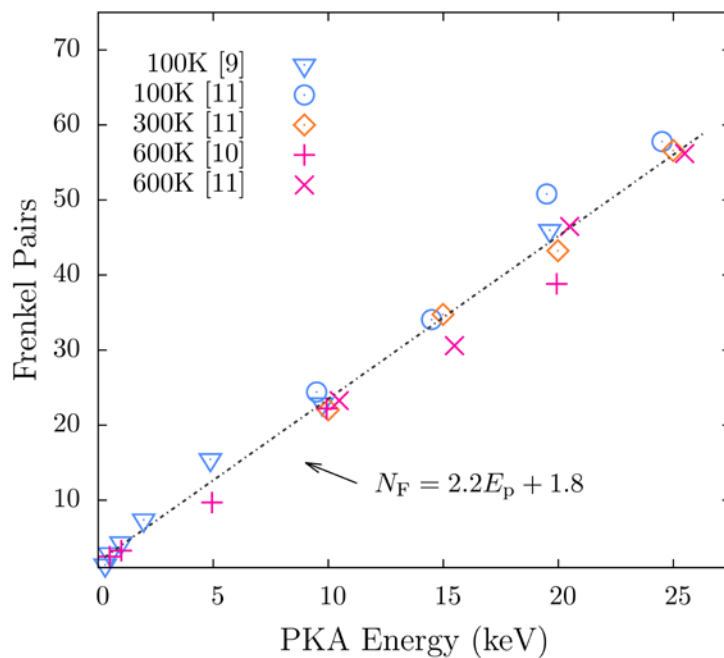


Fig. 1 The number of Frenkel pairs generated as a function of PKA energy for displacement cascades in α -Zr [9-11].

2. Simulation Methodology

Displacement cascades in α -Zr were simulated using LAMMPS, a molecular dynamics code distributed by Sandia National Laboratories [14, 15]. The simulation conditions consisted of seven bulk temperatures (15, 100, 200, 300, 400, 500 and 600 K) and seven PKA energies (0.5, 1.0, 5.0, 10.0, 15.0, 20.0 and 25.0 keV). For comparison with past studies, the AWB95 [12] interatomic potential was used. The simulation cell was built such that the crystal lattice was oriented with the $[11\bar{2}0]$ and $[0001]$ crystal directions parallel to the external X and Z directions. Periodic boundary conditions were used. The appropriate simulation cell size was scaled with PKA energy such that 88000, 181440, 380720, 802944, 1152576, 1540608 and 1702272 atoms per cell were used for the PKA energies listed above. Prior to conducting the cascade simulations, the cell energy was minimized using a conjugate gradient scheme. The simulation cell was then relaxed using an isothermal-isobaric ensemble at the simulation temperature of interest, with pressure equilibrated to zero. Displacement cascades, simulated using the statistics of the microcanonical ensemble, were initiated in the equilibrated cell by imparting a kinetic energy along the $[\bar{2}3\bar{1}9]$ crystallographic direction. This specific crystallographic direction was chosen as it has been reported to lead to representative behaviour [16]. In order to obtain better defect statistics, ten simulations were performed for each condition studied where a unique starting configuration for each repeat was obtained by allowing the system to run for a variable number of time steps in the microcanonical ensemble prior to cascade initiation.

Two defect identification methods were compared in this study. Both methods use a search radius r_c referenced to an initial lattice of atom sites. The first defect identification method uses a constant search radius of $0.32 a_o$, where a_o is the basal lattice constant at 0 K. This method is consistent with past studies [9-11, 17]. We develop an alternate method for defect identification which accounts for the lattice disturbance due to the presence of the irradiation defect and for thermal vibration. In this formalism, the search radius is given by,

$$r_c(T) = r_o(0) + r_T(T) \quad (2)$$

where r_o is associated with the displacement field of the irradiation defect at a temperature of 0 K and r_T is associated with atomic vibration in the undefected lattice at temperature T . The temperature independent component r_o was estimated from the equilibrium lattice displacement fields associated with various types of irradiation defects simulated at 0 K. The largest displacement from the reference lattice for atoms which are not defects, from the group of defects having low energy, was used to estimate r_o . Defect formation energies and their associated displacements, as described above, are shown in Table I for the irradiation defects relevant to the current simulations. Other recognized hcp defects are also considered but are not listed in Table I, as they relax to one of the listed defects. The basal triangular defect requires further description. This defect lies in the basal plane and is comprised of three self-interstitials surrounding a vacancy, forming a unit triangular structure. It is often observed in clusters on the basal plane [9]. The largest displacement from the group of irradiation defects having a formation energy less than 4.00 keV is 0.87 Å. This value is used for r_o .

Table I Defect formation energy E_f and displacement u_{\max} for irradiation defects that are commonly observed using the AWB95 interatomic potential.

Defect Type	E_f (eV)	u_{\max} (Å)
Basal crowdion	3.74	0.70
Basal octahedral	3.96	0.87
Basal triangular	6.86	0.82
Crowdion	3.97	0.43

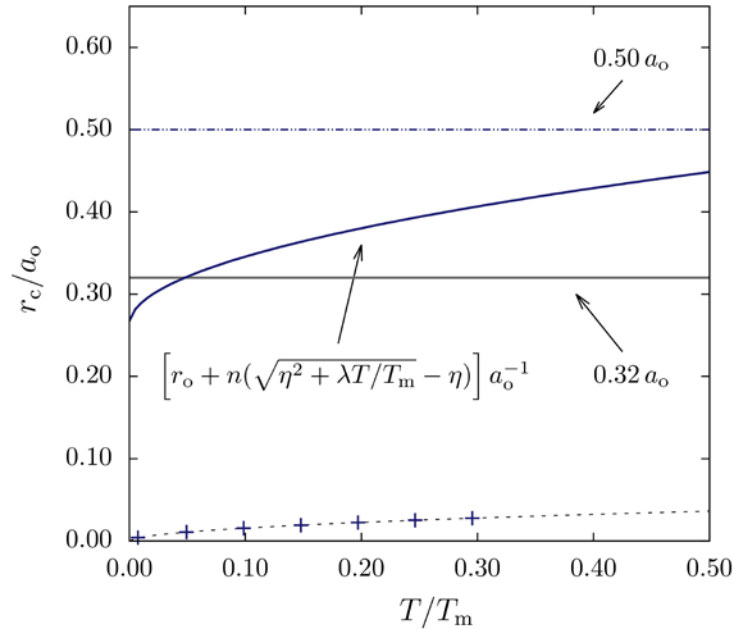


Fig. 2 Normalized search radius r_o/a_o versus homologous temperature T/T_m . The constant search radius of $r_c = 0.32 a_o$ and half the nearest neighbour distance $0.50 a_o$ are also shown for comparison. The + symbol represents the standard deviation of atom position measured relative to the closest reference atom site.

For an undefected crystal, the time-averaged atom position relative to the reference lattice follows a Gaussian distribution at temperature T . The standard deviation of atom position was found to follow a quadratic form with temperature, which leads to,

$$r_T = n \left[\sqrt{\eta^2 + \lambda T/T_m} - \eta \right] \quad (3)$$

where η and λ are material dependent constants, T/T_m is homologous temperature, and n is a parameter which can be related to the confidence interval of the Gaussian distribution. Parameters η and λ are obtained from fitting Eqn. (3) to the standard deviation of atom position versus temperature (Fig. 2) where atom position has been measured relative to the nearest atom reference site. A melting temperature T_m of 2030 K, obtained from the zirconium interatomic potential considered [12], was used. Values $\eta = 3.51 \times 10^{-3} \text{ \AA}$ and $\lambda = 2.93 \times 10^{-2} \text{ \AA}^2$ are obtained from the fit. Defect number and structure was analysed using a parametric study for which parameter n was varied from 1 to 10. Furthermore, when selecting an appropriate value for n , we also consider half the nearest neighbour distance to be an upper limit to r_c , which for zirconium is approximately $0.50 a_o$. Based on the above considerations, a value of $n = 5$ was chosen (see Fig. 2). Although the size of the simulation cell was chosen in part to limit the temperature rise due to the displacement cascade, the system temperature at the end of the simulation is observed to increase by 30 to 80 K. To account for this temperature increase, we calculate our search radius at $T + 100 \text{ K}$ when analysing data for an initial system temperature T .

3. Results and Discussion

Example defect data, generated at 15 and 600 K and analyzed using the temperature-dependent defect identification method, are shown in Fig. 3. Data for the Frenkel pair number for each particular cascade, the average number and the corresponding standard deviation are plotted as a function of the PKA energy (Fig. 3). The observed scatter is consistent with past studies [11]; the standard deviation of defect number increases in an approximately proportional fashion with E_p . The relative standard deviation of the Frenkel pair number was found to remain below 0.35 at all temperatures for PKA energies above 1 keV. The parameters defined in Eqn. (2) were therefore determined by using a weighted linear regression, where the weighting factor was taken to be the inverse of the relative standard deviation of the Frenkel pair number. Intercept N_o was found to be temperature independent and was set equal to 1.8 for all data sets analysed. For clarity, the compiled data is presented in Fig. 4 without error bars.

Defect identification using a constant search radius led to defect production statistics that were relatively temperature independent (Fig. 4 (a)). The number of defects was found to decrease slightly with temperature for a given PKA energy, which is consistent with the data presented in Fig 1. The largest difference, in an absolute sense, is observed at higher PKA energies. For example, at a PKA energy of 25 keV, the average number of Frenkel pairs generated is 180 at 15 K compared to 135 at 600 K. Parameter A , which measures the rate of defect generation with E_p , was found to decrease slightly with temperature from $A = 7.0$ at 0 K to $A = 5.5$ at 600 K. Nevertheless, the temperature dependence is small. If the data is taken to be temperature independent, the average value of A is equal to 6.5.

Temperature-dependent defect generation was observed when using the temperature-dependent defect identification search radius (Fig. 4 (b)). The temperature dependence, measured by the difference in the number of generated defects, is greatest at higher PKA energies. For example, at a PKA energy of 25 keV, the average number of Frenkel pairs generated is 175 at 15 K

compared to 74 at 600 K. The number of defects generated as a function of PKA energy was found to decrease in a systematic manner with temperature. Parameter A was found to decrease by factor of 2.3 over the temperature range studied, from $A = 7.0$ at 15 K to $A = 3.0$ at 600 K (Fig. 5). The trend can be captured by modifying Eqn. (1) to include the influence of temperature [18]. We propose a decay function for A such that,

$$A(T) = A_o + (A_s - A_o) \exp(-\xi/kT) \quad (4)$$

where k is the Boltzmann constant, A_o and A_s represent the rate of defect generation with E_p at 0 K and at the saturation temperature, respectively, and the apparent activation energy ξ determines the rate of decay of A with temperature where $\xi = \xi_H - \xi_S T$. The parameters associated with Eqn. (4) have been derived from the data presented in Fig. 5 and are given by $A_o = 7.0$, $A_s = 3.0$ and $\xi = 0.02 - 0.00003 T$ eV. Equation (4), plotted using the parameter values described above, is shown on Fig. 5. Equation (1), modified to account for temperature, is now given by,

$$N_F(T) = [A_o + (A_s - A_o) \exp(-\xi/kT)] E_p + N_o, \quad (5)$$

where E_p must be greater than about twice E_d . From Eqn. (5), the expression for a temperature-dependent defect production efficiency $\varepsilon(T)$, defined by the ratio of the stable number of Frenkel pairs observed from simulation over that predicted from the NRT model [13], is given by,

$$\varepsilon(T) = \frac{E_d}{0.4} \left[A(T) + \frac{N_o}{E_p} \right] \quad (6)$$

where E_d is usually taken to be temperature independent, although this assumption is questionable (see [19] for a discussion). The average temperature-independent threshold displacement energy for α -Zr is $E_d = 40.0$ eV [20]. Using this value, we re-evaluate parameter N_o by assuming that $\varepsilon(0) = 1.0$ at $E_p = E_d/0.4$. This condition leads to one Frenkel pair produced at the threshold displacement energy according to Eqn. (5). The re-analysis leads to $N_o = 0.03$, which, if used to re-evaluate A , does not have an appreciable influence on the trends observed in Fig. 5. The decrease in the defect production efficiency over the range of temperatures tested is independent of the PKA energy and is given by $\Delta\varepsilon = 0.40$.

Our results are at first surprising as our rate of defect generation is higher than that obtained from the previously published data for all conditions tested, even though we have used the same interatomic potential and, for the case of defect identification with a constant search radius, the same defect identification method. It is instructive to examine the results of Voskoboinikov et al. [11] in more detail. Their data was not included Fig. 1 as they use a cluster configuration analysis defect identification method. Details of this method are provided in their paper and will not be explained here. However, the difference between a critical search radius and cluster configuration analysis can be illustrated with a simple example. We consider a displacement

cascade that produced an isolated dumbbell, a concomitant vacancy somewhere in the vicinity, although not

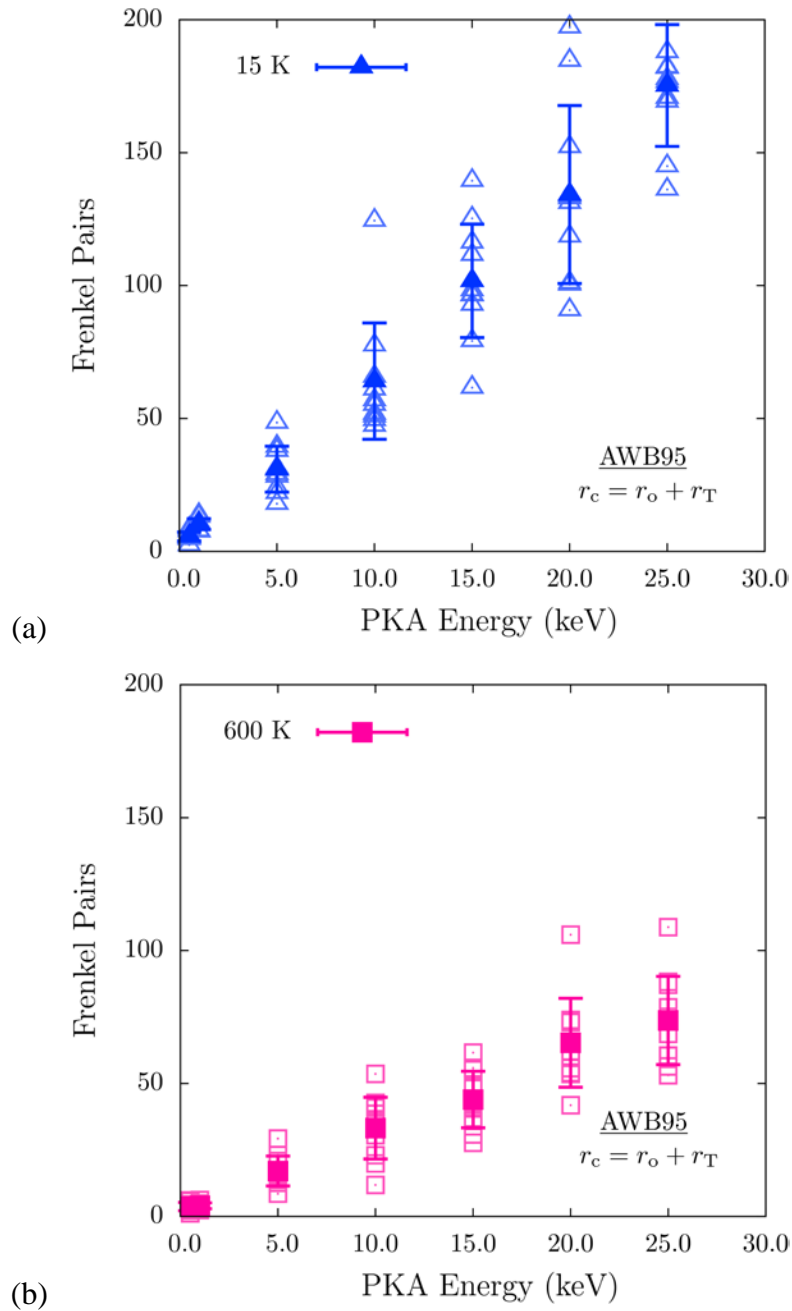
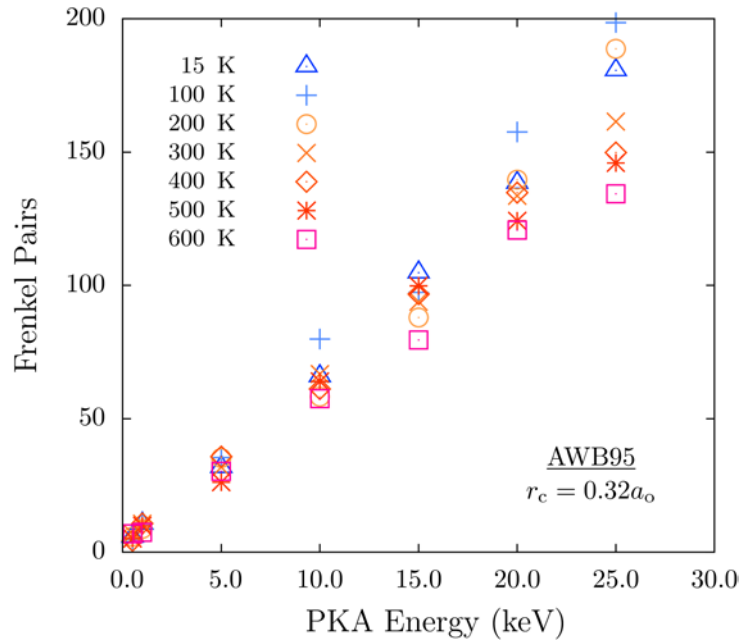
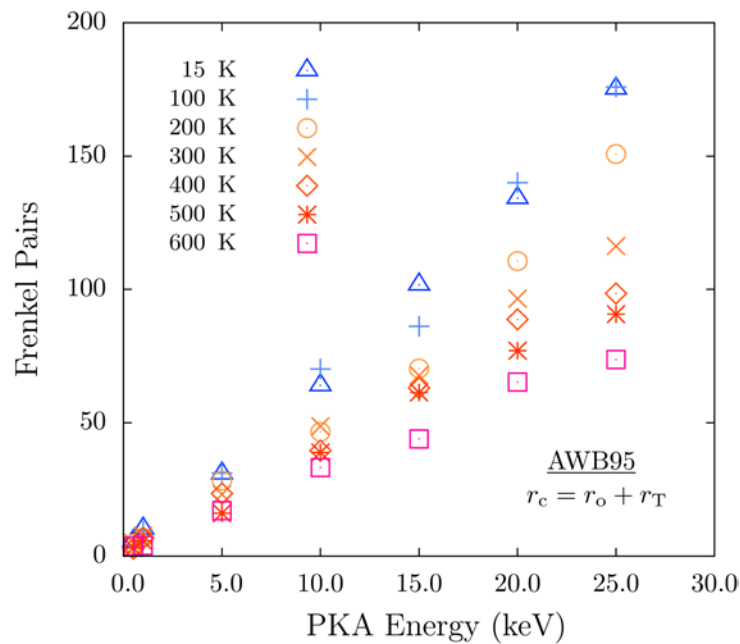


Fig. 3 The number of Frenkel pairs as a function of PKA energy for α -Zr displacement cascades measured using temperature-dependent defect identification at (a) 15 K and (b) 600 K. The open symbols represent data

for individual cascades, the closed symbols represent the average and the error bars are obtained from the standard deviation at a given PKA energy.



(a)



(b)

Fig. 4 The average number of Frenkel pairs as a function of PKA energy measured from α -Zr displacement cascades using a defect identification search radius that is (a) temperature-independent and (b) temperature-dependent.

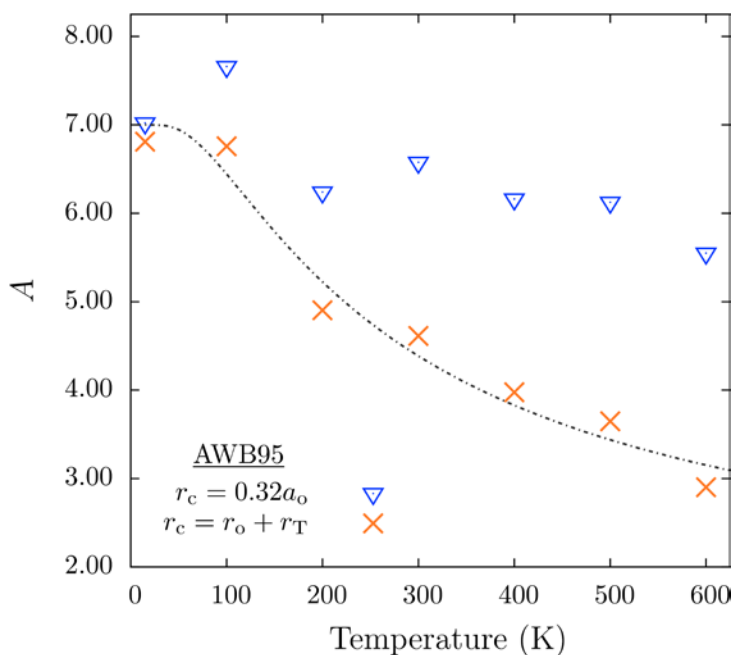


Fig. 5 Parameter A measures the rate of defect generation with E_p and is shown as function of temperature where it has been measured from defect statistics analyzed with both a temperature-independent and temperature-dependent defect identification search radius.

clustered with the dumbbell. The critical radius search method considers the isolated dumbbell defect as two self-interstitial atoms and one vacancy. Two Frenkel pairs are therefore counted. The cluster configuration analysis would count the isolated dumbbell as one self-interstitial atom and therefore, one Frenkel pair is counted. The cluster configuration analysis therefore results in fewer Frenkel pairs, especially when analysing clustered defect structures as commonly observed in α -Zr at high PKA energies. From a linear fit of the data of Voskoboinikov et al. [11], we obtain $A = 2.3$, and note that their rate of defect generation is lower and therefore, in this regards, qualitatively consistent with our data. However, as noted [11], the data of Voskoboinikov et al. is quantitatively consistent with the data of Bacon and co-workers [8-10]. However, this previously published data was analysed using a critical search radius of $0.32 a_o$, and therefore should exhibit higher defect counts than simulations analysed using the cluster

configuration analysis. Although Wooding and Bacon [8] use terminology such as di-interstitial to refer to a cluster with two excess interstitials (Fig. 9 in [8]), it is not clear if they use this classification when counting Frenkel pairs. Further research is required in order to identify the source of the observed differences.

The discrepancy between our temperature dependent results and previous studies can be attributed to the use of Eqn. (3) for defect identification. Justification for the new defect identification method lies in the need to account for the influence of kinetic energy on atom position when analysing data over a wide temperature range. With increasing temperature, the threshold for atomic displacement decreases and consequently, the size of the displacement cascade during the thermal spike phase increases. However, recombination efficiency increases with temperature, as higher temperatures facilitate the migration of point defects. The extent to which defect generation is influenced by temperature will depend on this competition, and therefore, in the molecular dynamics simulations, on the interatomic potential. An implication with regards to the analysis of in-core zirconium components is the addition of a source term for diffusion-induced creep processes, as temperature gradients are expected to lead to gradients in defect concentration.

4. Conclusions

Displacement cascade defect statistics were generated for α -Zr over a range of temperatures and PKA energies relevant to current and future fission nuclear reactors. A new approach for identifying interstitial defects, based on a temperature-dependent search radius, reveals that defect production in α -Zr is strongly temperature dependent. We find that the difference in the number of defects generated at low temperatures (15 K) compared to high temperature (≥ 600 K) is given by approximately four times the PKA energy. Based on the findings, a relation describing defect generation is proposed, which accounts for both temperature and incident recoil energy.

5. Acknowledgement

We wish to acknowledge the Office of energy Research and Development (OERD) at Natural Resources Canada (NRCan) for providing funding for this work.

6. References

- [1] G. B. Piercy, "Mechanisms for the in-reactor creep of zirconium alloys," *Journal of Nuclear Materials*, 26 (1), 1968, 18 – 50.
- [2] D. G. Franklin, G. E. Lucas, and A. L. Bement. *Creep of Zirconium Alloys in Nuclear Reactors*. ASTM Special Technical Publication 815, 1983.

- [3] R. A. Holt, G. A. Bickel, and N. Christodoulou, “Effect of fast neutron fluence on the creep anisotropy of Zr-2.5Nb tubes,” *Journal of Nuclear Materials*, 373 (1-3), 2008, 130 – 136.
- [4] M. Griffiths, “A review of microstructure evolution in zirconium alloys during irradiation,” *Journal of Nuclear Materials*, 159 (0), 1988, 190 – 218.
- [5] V. Fidleris, R. P. Tucker, and R. B. Adamson, “An overview of microstructural and experimental factors that affect the irradiation growth behavior of zirconium alloys,” In *Zirconium in the Nuclear Industry: Seventh International Symposium*, ASTM STP 939, pages 49 – 85, Philadelphia, 1987.
- [6] R.A. Holt, “Mechanisms of irradiation growth of alpha-zirconium alloys,” *Journal of Nuclear Materials*, 159 (0), 1988, 310 – 338.
- [7] A. Rogerson, “Irradiation growth in zirconium and its alloys”, *Journal of Nuclear Materials*, 159 (0), 1988, 43 – 61.
- [8] S. J. Wooding and D. J. Bacon, “A molecular dynamics study of displacement cascades in α -zirconium,” *Philosophical Magazine A*, 76 (5), 1997, 1033–1051.
- [9] S. J. Wooding, L. M. Howe, F. Gao, A. F. Calder, and D. J. Bacon, “A molecular dynamics study of high-energy displacement cascades in α -zirconium,” *Journal of Nuclear Materials*, 254 (2-3), 1998, 191–204 .
- [10] F. Gao, D. J. Bacon, L. M. Howe, and C. B. So, “Temperature-dependence of defect creation and clustering by displacement cascades in α -zirconium,” *Journal of Nuclear Materials*, 294 (3), 2001, 288 – 298.
- [11] R. E. Voskoboinikov, Y. N. Osetsky, and D. J. Bacon., “Atomic-scale simulation of defect cluster formation in high-energy displacement cascades in zirconium,” *Journal of ASTM International*, 2 (9), 2005, 229–243.
- [12] G. J. Ackland, S. J. Wooding, and D. J. Bacon, “Defect, surface and displacement-threshold properties of α -zirconium simulated with a many-body potential,” *Philosophical Magazine A*, 71 (3), 1995, 553–565.
- [13] M. J. Norgett, M. T. Robinson, and I. M. Torrens. A proposed method of calculating displacement dose rates. *Nuclear Engineering and Design*, 33 (1), 1975, 50 – 54.
- [14] S. J. Plimpton. Fast parallel algorithms for short-range molecular dynamics. *Journal of Computational Physics*, 117, 1995, 1–19.
- [15] <http://lammmps.sandia.gov>.
- [16] S. J. Wooding, D. J. Bacon, and W. J. Phythian, “A computer simulation study of displacement cascades in α -titanium,” *Philosophical Magazine A*, 72 (5), 1995, 1261–1279.

- [17] R. E. Voskoboinikov, Y. N. Osetsky, and D. J. Bacon, “Statistics of primary damage creation in high-energy displacement cascades in copper and zirconium,” *Nuclear Instruments and Methods in Physics Research Section B: Beam Interactions with Materials and Atoms*, 242 (12), 2006, 68–70.
- [18] K. P. Boyle and I. Shabib. Temperature dependence of defect production efficiency in α -Fe. In *5th International Symposium on Supercritical Water-Cooled Reactors*, page 55, Vancouver, BC, Canada, March 14-16 2011.
- [19] P. Vajda, “Comment on "Molecular dynamics study of the threshold displacement energy in vanadium",” *arXiv:cond-mat/0403275*, 2004.
- [20] C. H. M. Broeders and A. Yu. Konobeyev, “Defect production efficiency in metals under neutron irradiation,” *Journal of Nuclear Materials*, 328 (2-3), 2004, 197–214.